Improving Net Joint Torque Calculations Through a Two-Step Optimization Method for Estimating Body Segment Parameters

Raziel Riemer
Ph.D.
Department of Industrial Engineering and Management,
Ben-Gurion University,
Beer-Sheva 84105, Israel

Elizabeth T. Hsiao-Wecksler[1]
Ph.D.
Department of Mechanical and Science Engineering,
University of Illinois at Urbana-Champaign,
MC-244,
1206 West Green Street,
Urbana, IL 61801
e-mail: ethw@uiuc.edu

Two main sources of error in inverse dynamics based calculations of net joint torques are inaccuracies in segmental motions and estimates of anthropometric body segment parameters (BSPs). Methods for estimating BSP (i.e., segmental moment of inertia, mass, and center of mass location) have been previously proposed; however, these methods are limited due to low accuracies, cumbersome use, need for expensive medical equipment, and/or sensitivity of performance. This paper proposes a method for improving the accuracy of calculated net joint torques by optimizing for subject-specific BSP in the presence of characteristic and random errors in motion data measurements. A two-step optimization approach based on solving constrained nonlinear optimization problems was used. This approach minimized the differences between known ground reaction forces (GRFs), such as those measured by a force plate, and the GRF calculated via a top-down inverse dynamics approach. In step 1, a series of short calibration motions was used to compute first approximations of optimized segment motions and BSP for each motion. In step 2, refined optimal BSPs were derived from a combination of these motion profiles. We assessed the efficacy of this approach using a set of reference motions in which the true values for the BSP, segment motion, GRF, and net joint torques were known. To imitate real-world data, we introduced various noise conditions on the true motion and BSP data. We compared the root mean squared errors in calculated net joint torques relative to the true values due to the optimal BSP versus traditionally-derived BSP (from anthropometric tables derived from regression equations) and found that the optimized BSP reduced the error by 77%. These results suggest that errors in calculated net joint torques due to traditionally-derived BSP estimates could be reduced substantially using this optimization approach. [DOI: 10.1115/1.3005155]

Keywords: inverse dynamics, optimization, joint moments, error reduction

1 Introduction

Inverse dynamics is a procedure commonly used in the biomechanical analysis of human movement. This procedure calculates force and net torque reactions at various body joints using anthropometric, kinematic, and kinetic input data [1]. Uncertainty in estimated net joint torques derived from this method can, however, range from 6% to 232% of the peak net torque [2]. This uncertainty depends on measurement and/or estimation errors of the input parameters to the inverse dynamics expressions. Main contributors to these uncertainties were identified to be inaccuracies in estimated segment angles and body segment parameters (BSPs) [2]. Errors in segment angular data arise from two main sources: noise in the motion-capture system and movement artifacts of skin-mounted markers [2,3]. Inaccuracies in body segment parameters are due to errors in estimating segmental mass, moment of inertia, and center of mass (COM) location [2,4–7].

Several methods have been proposed for estimating BSPs. Commonly used to estimate BSP are weighting coefficients based on regression equation relationships derived from measurements on cadavers or living subjects [8–11]. These coefficients relate subject height and weight to the BSP. Error due to estimations based on cadaveric data may exceed 40% [4]. Errors based on living-subject data are smaller than cadaveric data, but are still considered relatively high [10]. Geometric approaches [12,13] estimate body segment shapes and use estimated density to calculate BSP. These approaches may produce smaller errors (e.g., less than 5% [12]), but achieving such accuracy is cumbersome as it requires large numbers of measurements per subject (between 90 [13] and 248 [12]). Methods based on medical imaging (e.g., Refs. [14,15]) have high accuracy (errors of 5% or less). These methods, however, need medical imaging equipment that is not always available and additionally expose subjects to radiation. Recently, a technique for identifying arm BSP based on arm kinematics and manipulator-hand contact forces was proposed [16].

Another approach that used external forces for estimating BSP was proposed by Vaughan et al. [17]. This method used the overdetermined nature of the inverse dynamics approach to formulate a nonlinear optimization problem. This overdeterminancy is explained as follows. Traditionally, two approaches have been used for inverse dynamics computations. The first requires only kinematic and anthropometric data to calculate net joint torques. Referred to as the top-down approach, this process often starts at the distal segment of the upper extremity(ies) and proceeds downward such that dynamic equilibrium conditions are satisfied for each

[1]Corresponding author.

Contributed by the Bioengineering Division of ASME for publication in the JOURNAL OF BIOMECHANICAL ENGINEERING. Manuscript received December 1, 2007; final manuscript received September 22, 2008; published online November 20, 2008. Review conducted by Mohamed Samir Hefzy. Paper presented at the 31st Annual Meeting of the American Society of Biomechanics, Stanford, CA, August 22–25, 2007.

successive segment. The second method, or the bottom-up approach, is typically used to analyze locomotor tasks and uses ground reaction force (GRF) measurements. This method starts at the distal segment of one or both of the lower extremities and proceeds upward through the body. By incorporating GRF measurements, boundary conditions are defined for the bottommost segment. These added conditions result in an overdetermined system since there are now more equilibrium equations than system unknowns [17–19]. Due to errors in input parameters to the inverse dynamics calculations, these traditional methods result in residual forces and torques on the most-distal segment. The propagation of systematic errors typically limits either method to proximal net joint torque calculations; however, if it was possible to mitigate the effects of one or more of these input inaccuracies, improvements in net torque calculations (for all joints) could be achieved.

This overdeterminancy has been used to reduce error effects through optimization methods that adjust specific input parameters in the top-down calculations [17–19]. To improve subject-specific BSP estimates, Vaughan et al. [17] formulated an optimization problem that minimized the residuals between the known ground reaction measurements and those predicted through the top-down calculation. This promising method, proposed in 1982, failed to gain popularity due to the complexity and high computing demands of solving an optimization problem. Newer computing capabilities have reduced these difficulties. Another weakness of this work was that they did not account for errors in the motion data. Furthermore, Vaughan et al. assumed that minimizing a cost function is sufficient for reducing the net joint torque calculation error. Their cost function did not contain information on the net joint torques; therefore, it is possible to minimize the cost function while simultaneously increasing error in the net joint torques. In an effort to minimize errors due to noise in measured data (i.e., GRF measurements and segment motion), Kuo [19] overcame this problem by suggesting an additional success criterion. This criterion stated that the difference between the true net joint torque and the torque determined from the optimized solution should be less than the difference between the true and traditional (nonoptimized) inverse dynamics solution. Delp et al. [20] recently proposed the use of slight controlled adjustments to kinematic and mass parameters to reduce the residual between measured and calculated GRFs; however, this approach was used to create better simulations of human movement rather than used to determine experimental net joint torques.

This paper describes a method that used the overdetermined nature of the inverse dynamics approach to find an optimal set of subject-specific BSP estimates that reduce the error in joint net torques (due to inaccurate BSP estimation), while accounting for errors in motion data measurements. The premise of our approach is that a test subject/patient would perform a series of calibration motions, which would be used to derive optimized subject-specific BSPs. Once these BSPs are determined, then they can be used in inverse dynamics calculations for any desired task motion performed by the subject. The long-term goal of our work is to develop a method to increase the accuracy of joint net torque calculations through improvements of estimates for both BSP and segment motions using optimization techniques.

2 Method

The approach proposed in the current study was inspired by optimization methods used by Vaughan et al. [17], Cappozzo [21] and Mazza and Cappozzo [22]. As noted previously, Vaughan et al. [17] used GRF data to compute optimal BSP estimates, but their method breaks-down when motion data errors are present. Cappozzo [21] and Mazza and Cappozzo [22] used GRF data to compute optimal solutions for joint angular motion, but did not address errors in BSP. Our optimization method builds from these works and uses a two-step sequential approach to determine a set of optimal BSP estimates that improve net joint torque accuracy.

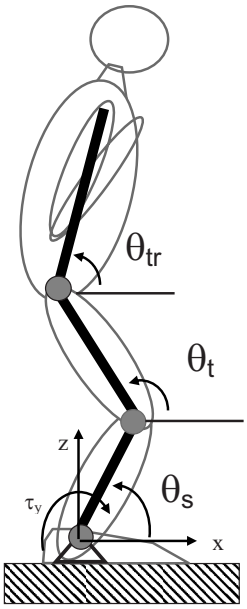

Fig. 1 The body represented by a three-segment model. Segment angles for the shank (θ_s), thigh (θ_t), and torso (θ_{tr}) were defined as shown.

To summarize our approach, the optimization cost function was based on the difference between the measured ground reaction forces and the GRF calculated using top-down inverse dynamics (see Sec. 2.1). Since optimization performance depends on having sufficient information of the system, a set of three short calibration motions was used to increase the likelihood of having sufficient data to identify the optimal BSP. To test the efficacy of our method, we derived a set of reference motions in which the true values for the BSP and angular profiles were known (see Sec. 2.2). In this case study, we applied the inverse dynamics method to planar symmetric motions and solved for the net joint torques and ground reaction forces. The human body was modeled as a rigid body system (Fig. 1). The results from the optimized BSP were then compared to nonoptimized BSP results.

2.1 Optimization Formulation. The general formulation for the optimization problem was

$$\min z(\nu) \quad \text{subject to} \quad \begin{cases} c_k(\nu) = 0, & k \in E \\ c_k(\nu) \geq 0, & k \in I \end{cases} \tag{1}$$

where z is the objective function, $c_k(\nu)=0$, $k \in E$ are equality constraints, $c_k(\nu) \geq 0$, $k \in I$ are inequality constraints, and ν is a vector of optimization variables (i.e., segment angles and BSP). The objective function was the least square of the difference between the calculated forces obtained with a top-down approach and the known GRF. Therefore, the 2D objective function was

$$z = \sum_{i=1}^{n} [(f_i^x(\nu) - \bar{f}_i^x)^2 + (f_i^z(\nu) - \bar{f}_i^z)^2 + (\tau_i^y(\nu) - \bar{\tau}_i^y)^2] \tag{2}$$

where i is the time index, n is the total number of time intervals during the chosen motion, f^x, f^z, and τ^y are the calculated ground reaction forces and net torque (using a top-down approach) as a function of the optimization variables ν, and $\bar{f}^x$, $\bar{f}^z$, and $\bar{\tau}^y$ are the known ground reactions (i.e., "true" values when considering an idealized perfect system or "measured" values when considering a real-world experimental system). Directions x, y, and z are defined in Fig. 1. The equations of motion used to calculate the net joint torques and ground reaction values were derived using the gener-

alized coordinate approach [19].

The objective function was minimized under two types of constraints: (1) motion constraints on the angular profiles and (2) body segment parameter constraints. Both of which are detailed below.

2.1.1 Motion (Angular Profile) Constraints. Equality motion constraints were used to calculate the angular velocity and acceleration of each segment. These values were obtained using the central finite difference method. The inequality motion constraints apply only to step 1 because in that step the optimization manipulates the angular profiles, whereas the combined motion profile in step 2 is not optimized. Inequality constraints on the angular positions limited the optimized values to be within the upper and lower bounds:

$$\bar{\theta}_{i,j} + \varepsilon_a \geq \theta_{i,j} \geq \bar{\theta}_{i,j} - \varepsilon_a \tag{3}$$

where $\bar{\theta}_{i,j}$ is the measured angle, $\theta_{i,j}$ is the optimized value, and j is the segment index. ε_a is the maximum possible error in the known angle and can be derived by examining skin movement artifacts [23–25]. In this study, we used 0.035 rad, 0.07 rad, and 0.07 rad for the shank, thigh, and head-arm-torso (HAT) segments, respectively.

An additional inequality constraint provided bounds on angular acceleration. This constraint was expressed in the following form:

$$\ddot{\bar{\theta}}_{i,j} + \varepsilon_{\text{acc}} \leq \ddot{\theta}_{i,j} \leq \ddot{\bar{\theta}}_{i,j} - \varepsilon_{\text{acc}} \tag{4}$$

where $\ddot{\bar{\theta}}$ is the measured value for the angle acceleration, $\ddot{\theta}$ is the optimized value, and ε_{acc} is the maximum acceleration error. This upper bound for the acceleration error is not well documented in literature, and as such, we used estimations from Ref. [2] and estimations based on studies that evaluated errors due to the skin movement artifact [23–25] and the motion-capture system [26]. In this study, we used 1.3 rad/s^2, 1.8 rad/s^2, and 2.5 rad/s^2 for the shank, thigh, and HAT segments, respectively.

Another inequality constraint was based on the kinematic configuration, such that errors in the location of each joint center had to fall within a specified range ε_k. The error was defined as the difference between the joint center location determined from the motion-capture system measurement $(\bar{x},\bar{z})$ and the location predicted by the link length (L_j) and optimized segment angle $(\theta_{i,j})$. For 2D, these constraints take the following form:

$$\varepsilon_k \geq \left[\bar{x}_{i,k} - \sum_{j=1}^{k} L_j \cos(\theta_{i,j})\right]^2 + \left[\bar{z}_{i,k} - \sum_{j=1}^{k} L_j \sin(\theta_{i,j})\right]^2 \tag{5}$$

where k is the joint number. ε_k was derived from joint center studies [27–30]. In this study, we used ε_k of 0.0005 m for ankle to knee, 0.0012 m for ankle to hip, and 0.001 m for ankle to shoulder.

2.1.2 Body Segment Parameter Constraints. Body segment parameter constraints were applied in cases when BSPs were variables in the optimization (i.e., steps 1 and 2). Upper and lower BSP bounds, which represent the maximum possible error in the given parameter, were defined with the following inequality constraints:

$$\bar{P}_l + \varepsilon_l \bar{P}_l \geq P_l \geq \bar{P}_l - \varepsilon_l \bar{P}_l \tag{6}$$

where $\bar{P}_l$ is the initial estimate for a body segment parameter, P_l is the optimized value, and ε_l is the percent of possible error in the lth BSP. The values for ε_l were based on error estimations from past studies [5–7] and are presented in Table 1. The body was assumed to be bilaterally symmetrical for all BSPs. In addition, we added the following equality constraints to conserve the total mass:

Table 1 Percentage of error in BSP estimations for each segment relative to the true value. The values for the COM location and moment of inertia represent the maximum possible error for each segment. Errors in segment mass must maintain the total body mass as per Eq. (7).

Segment	Mass	COM location	Moment of inertia
Head+torso	5	12	10
Arm	10	6	4
Thigh	10	2	15
Shank	1	17	3

$$\text{total body mass} = \sum_{l=1}^{p} \bar{m}_l = \sum_{l=1}^{p} m_l \tag{7}$$

where $\bar{m}_l$ is the initial estimation for mass segments, m_l is the estimation after the optimization, and p is the number of segments.

2.1.3 The Sequential Optimization Approach. Our earlier work focused on reducing the effect of error in the motion data (segment angular positions, velocities, and accelerations) by optimization of segment angular data [31]. In that work, we found that compared to traditional nonoptimized approaches, the optimization approach reduced angular error in the motion data by 27–62%. This reduction in angular error translated into a reduction in net joint torque error by 54–79% (see Figs. 3 and 4 in Ref. [31]). In the current work, we use a two-step sequential approach to extend that work to enable optimization of both segment angles and BSP estimates (Fig. 2).

In step 1, we used each calibration motion individually to derive first approximations for the optimal BSP and motion profiles. That is, the optimization variables ν were the segment angular position profiles (2D flexion-extension angles at each sampling point) and the BSP (segmental COM location, mass, and moment of inertia relative to the distal joint axis) for the shank, thigh, and HAT segments. All parameters were manipulated concurrently to minimize the difference between the calculated and measured GRFs. Note that in this study we assume that after filtering we can neglect measurement/equipment error inherent in GRF. Step 1 was performed separately for three short calibration motions. To start the optimization procedure, initial guesses for each motion and the BSP were derived from the angular profiles calculated from the raw marker data and from estimations for BSP based on anthropometric charts [32].

In step 2, a further refined set of BSP was derived from a motion profile created from a combination of the optimized calibration motions. This is because currently we can only optimize for a few seconds of motion at a time; longer times (i.e., more data) would require greater computation time for solving an optimization problem that accommodates for both motion and BSP. Thus, step 2 further optimizes only the BSP. To create the combined motion, the first and last 20 ms of each motion were eliminated prior to concatenation. This approach was used since our optimization procedure for angular profiles [31] was found to have higher end-effect errors since there are no boundary condition constraints at these points. The BSPs derived from one of the calibration motions in step 1 (BSP1) were used as the initial BSP guess for step 2. The BSP estimates were then optimized under the BSP constraints (Eqs. (6) and (7)) while the angular profiles remained fixed. (Note that one could use BSP1 as obtained from any of the three motions.)

Our formulation for the optimization-based inverse dynamics approach was solved in step 1 using the SNOPT (large-scale sequential quadratic programming (SQP)-based nonlinear programming (NLP) solver from Stanford University) and executed using the general algebraic modeling system (GAMS) (Washington,

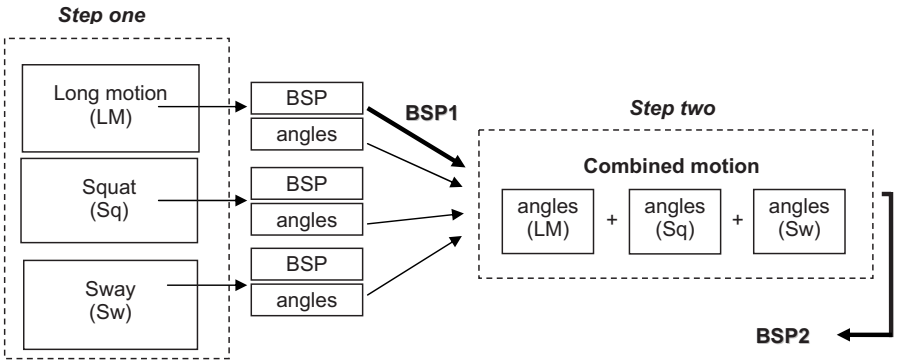

Fig. 2 Two step sequential optimization approach to determine optimal subject-specific body segment parameters (i.e., center of mass location, mass, and moment of inertia) in the presence of motion data error. Step 1 finds preliminary optimized BSPs and angular profiles that minimize the objective function; this step is done for the three different calibration motions. In step 2, the optimized angular profiles found in step 1 are concatenated together and BSPs from one of the three motions (BSP1) are used to find a refined second estimation (BSP2).

DC), which is a high-level modeling and optimization package. In step 2, the optimization problem was solved using a constrained nonlinear optimization function (fmincon function, MATLAB; The MathWorks, Inc., Natick, MA, Version 6.5). The optimization in step 2 is relatively simple, and therefore for convenience reasons, we chose to use this solver.

All BSP optimization variables in either step were considered to be independent. Note that in this formulation (COM location, mass, and moment of inertia), BSP estimates do not result in a unique solution. In addition, we tried a formulation that correlated mass (m) to moment of inertia (I) using the equation $I_i=k_i^2 m$, where k_i is the radius of gyration for segment i. However, this formulation does not provide a unique solution as it still tries to fit three parameters for each segment (i.e., COM location, mass, and now radius of gyration—instead of moment of inertia). Furthermore this formulation was computationally heavier to solve. The only formulation that we have identified that could have a single solution was if we assumed that each link could be represented by a point mass approximation. In this case, there are only two independent variables (mass and distance from the point mass to the axis of rotation) per segment. This formulation would make the solution unique; however, it would add overall error due to the point mass approximation.

2.2 Assessment of the Optimization Methodology (Evaluation Framework). Since in actual experimental settings true joint net torque and BSP values are never known, we used the following framework to evaluate the performance of our optimization-based method (Fig. 3). In the first phase, we constructed an ideal error-free system of reference motions to use as test data. These data created sets of true (noise-free) anthropometric BSP data and true segment angle profiles for each motion. These data were then entered into top-down inverse dynamics calculations to obtain true values for the net joint torques and GRF for each motion. In the second phase to simulate real experimental situations, errors (dotted entities) were introduced to the true BSP and angular profiles,

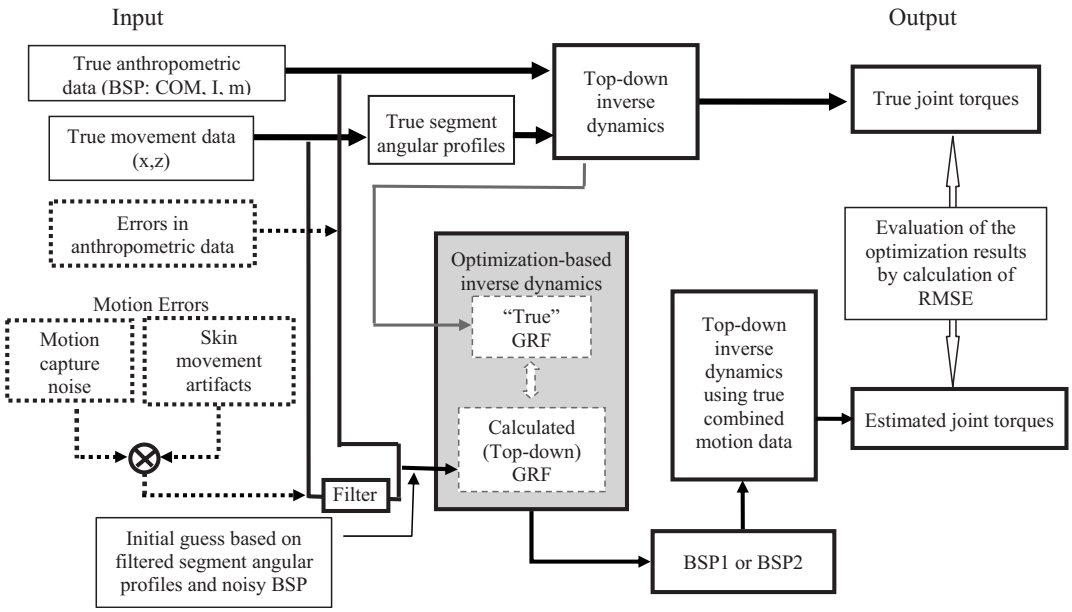

Fig. 3 Framework for performance evaluation of the proposed method to determine the efficacy of optimized BSP estimates in calculating net joint torques. Note that the gray box corresponds to the sequential optimization described in Fig. 2.

which were then digitally filtered. These motion and BSP values were then used as initial guesses for the step 1 optimizations. In the third phase, we solved for optimal angle profiles and BSP estimates (BSP1 or BSP2) (Sec. 2.1.2). For the optimization, the true GRFs used in the objective function were derived from the top-down inverse dynamics solution of the true data. Finally, to test the efficacy of the approach, in the fourth phase the net joint torque results from the different estimates of the BSP during the optimization were compared to the true values.

This method was implemented on a case study that focused on the 2D motion of a three-segment (head-arm-torso, thigh, and shank) system. For this system, we assume that the true values (i.e., BSP, joint center coordinates, segment angular profiles, GRF, and net joint torques) for a set of calibration motions were known. The motions for the segment angle profiles were derived from one individual (height of 1.8 m, mass of 80 kg) performing four planar sagittal motions at natural speed and builds upon previous studies that used this technique [19,31]. All motions were performed with the arms across the chest. The three calibration motions were (1) a long motion that involved a single cycle of flexion and hyperextension of the hips followed by flexion and extension of the knees, (2) a squat motion, and (3) a sway motion. In addition to the calibration motions, the test subject preformed a torso leaning motion, where he flexed his torso forward to an approximately 45 deg angle and then returned to an erect posture. The last motion was used to assess the effect of the optimized BSPs on a motion other than the calibration motions. Segment angle profiles for all motions were derived from motion data initially captured using a six-camera Vicon system (model 460, Vicon Peak, Lake Forest, CA) at a sampling rate of 100 Hz. To create the true segment angle profiles, baseline analytical profiles were derived by fitting the angular profiles from the motion-capture data to a 15th order polynomial function (polyfit function, MATLAB; The MathWorks, Inc., Natick, MA, Version 6.5). Using these profiles, the net joint torques and GRF were computed using a top-down inverse dynamics approach. To more closely simulate real-life experimental procedures, 2D coordinate data (x,z) for the joint center locations were generated from the baseline angular profiles combined with the kinematic constraints imposed by using a three-segment model with defined segment lengths. This step simulated the use of motion-capture marker data to identify joint center locations.

Next, error was introduced into these idealized true coordinate data (x,z). Error based on skin movement artifacts was simulated by a sinusoidal noise model derived from prior models in literature (e.g., Refs. [29,33–35]). The model parameters were set such that segment angular error was similar to measurement error, as reported in literature (e.g., Refs. [23–25]). Noise in the motion capture system was simulated using zero-mean white noise [19,29,33,34] with a standard deviation of 0.60 mm [26].

Errors in the BSP were introduced using a two stage procedure. In the first stage, errors were introduced to the body segment masses. Error in the head-torso segment mass was set to either +5% or −5% of the segment mass. The remaining difference between the true and the new mass of the head-torso segment was then distributed to the other body segments based on the premise that the mass of the head-torso is approximately 60% of the total body mass and would therefore dictate the rest of the segmental mass errors. Based on this assumption and error estimates taken from literature for other body segments, error was, respectively, set to −10% or +10% of the segment mass in the arm and thigh segments and −1 or +1% segment mass in the shank (Table 1). Total body mass remained constant as per Eq. (7). Using this approach, there could be two types of error: (1) the mass of the head-torso was heavier than the true value and the arms and legs were lighter, and (2) the opposite (head-torso lighter and legs-arms heavier). In the second stage, errors were randomly introduced into each segment's center of mass location and moment of inertia. The maximum possible errors in each of these BSP estimates are presented in Table 1. Error magnitudes were selected from maximum error values reported in past studies [5–7].

Ten noise conditions, randomly assigned within the error boundaries defined in Table 1, were applied to the BSP values (simulating ten different test subjects of slightly different physique). Randomly-assigned motion noises were applied to each of the calibration motions simulating the noise conditions that would be expected when each "test subject" performed the three motions. After the errors in angular motion profiles and BSP estimates were introduced, the optimization problem was solved using the sequential approach.

2.3 Data Analysis. To examine the efficacy of the two-step sequential approach, a number of assessments were performed. First, convergence of the optimization algorithm was verified, and the average root mean square error (RMSE) between the true and calculated GRFs was checked. Second, we wanted to understand how variations in only the BSP affected the inverse dynamics solutions (Fig. 3); therefore, we inserted the estimated BSP from different points in the optimization (initial guess, post-step-1 (BSP1) or post-step-2 (BSP2)) into top-down inverse dynamics calculations that used the noise-free motion profiles. We then compared the net joint torques derived from the noise-free BSP values to the net torques derived from these BSP estimates. These net joint torques were used to compute the RMSE over all joints for a given motion at each step. Third, since in nonlinear optimizations the initial conditions (guess) can affect the solution of the optimization, we tested whether using different BSP from step 1 (BSP1) as the initial guess for step 2 would affect the net joint torque results. The different BSPs were obtained from each calibration motion, and the effect of these different initial conditions was evaluated by comparing the average RMSE of all net joint torques after step 2. Last, we used the torso leaning motion to assess if the BSP obtained using the optimization (BSP2 after step 2) reduced the joint torque error due to BSP error. For this case, BSP1 from the long motion were used as the initial guess to determine BSP2.

3 Results

First, for all trials, the optimization algorithm converged, and for step 1 it always reduced the difference between the true GRF and the calculated GRF to RMSE values of less than 0.02 N (or 0.02 N m for the ground reaction ankle moment). Second, Table 2 presents the average differences in net joint torques (RMSE) between the true values and values obtained using the estimated BSP at each step of the optimization (i.e., RMSE due only to BSP). Comparisons between before and after step 1 values show an average reduction in the RMSE of 76.6%, 52.4%, and 56.3% for the individual long, squat, and sway motions, respectively. For the combined motion, an overall reduction of approximately 77% was found when comparing the RMSE of the nonoptimized (initial) noisy values to the more refined BSP estimated after step 2 (BSP2). Third, we found that using BSP1 values obtained from different motions as the initial guess for step 2 had a substantial effect on the net joint torque RMSE after step 1, but little effect after step 2. That is, the average reduction in RMSE from step 1 to step 2 was 11% for the long motion, but 46–47% for the sway and squat motions; however, the overall improvement between initial and step 2 results (~77%) differed by less than 1% for all three sources of BSP1. Last, a fourth unrelated motion (torso leaning) was evaluated. Comparison between initial noisy values to results using BSP2 found an average reduction in RSME of 69%.

4 Discussion

This paper proposes a method for improving the accuracy of calculated net joint torques by computing optimized anthropometric BSP estimates in the presence of motion-capture noise. The concept of estimating BSP using GRFs was previously proposed

Table 2 Average torque RSME compared to true noise-free values across all joints due to different BSP noise conditions and using BSP estimates from different points in the optimization procedure (nonoptimized (initial) noisy values, post-step-1 (BSP1) or post-step-2 (BSP2)). See Fig. 3.

Noise condition No.	Long motion (N m)		Squat (N m)		Sway (N m)		Combined motion (N m)[a]			Torso leaning (N m)[a]	
	Initial	BSP1	Initial	BSP1	Initial	BSP1	Initial	BSP1	BSP2	Initial	BSP2
1	17.11	3.90	10.44	2.01	16.81	1.81	17.88	4.82	2.32	3.13	1.87
2	8.82	3.41	5.45	0.66	9.83	5.16	8.84	3.04	3.36	5.15	2.91
3	1.22	2.38	0.95	4.07	1.69	2.47	1.39	2.43	1.65	0.77	1.65
4	27.87	2.32	14.29	0.89	23.98	3.75	24.28	2.18	2.36	19.45	1.58
5	7.47	3.88	4.40	6.44	7.01	5.53	6.88	3.79	1.58	5.01	1.51
6	19.44	3.90	12.07	5.46	17.79	7.24	17.88	4.28	4.03	13.22	4.34
7	1.34	1.42	0.80	1.45	0.78	4.16	1.02	1.68	2.12	1.34	1.87
8	17.52	2.34	9.66	3.05	13.81	4.91	14.91	2.22	2.84	13.01	2.00
9	10.50	2.64	6.16	0.98	9.34	5.40	9.45	2.16	3.02	7.32	2.31
10	8.13	1.63	0.80	5.95	0.78	4.02	6.42	1.53	1.85	1.34	1.81
Average	11.94	2.78	6.50	3.10	10.18	4.44	10.89	2.81	2.51	6.97	2.19

[a]Results for the combined motion used BSP1 values derived from the long motion.

by Vaughan et al. [17]; however, that method was not validated and not designed to account for characteristic motion data errors (i.e., skin movement artifacts). In contrast, our sequential approach was able to accommodate and optimize BSP calculations even when errors existed in the motion data. Furthermore, by adding the second optimization step (step 2), reduction in net joint torque error shows improvement (11–47%) compared to results obtained if only one optimization step was performed. These findings highlight the utility of our multistep approach for improving torque calculations. Comparing noisy initial guess values for BSP to final post-step-2 optimized set of BSP (BSP2), we found that the error in net joint torques due to BSP inaccuracies was reduced by 77% (average RMSE over all joints). Moreover, when these BSP2 values were used on a new motion (torso leaning), a reduction in net joint torque of 69% was also achieved.

It should be noted that, although an optimized set of BSP was found that minimized the error in the net joint torques (which was our main concern), these BSP estimates are not a unique set and cannot be considered the true BSP values for each segment. Block and Spong had similar findings in their investigation of a two link robotic arm [36]. Our pilot work suggests that, when the true value for one BSP is given and the other two are manipulated by the optimization, the true values for these two parameters can be determined. This finding indicates that if we can determine one of the parameters with high accuracy using a different method, it would be possible to use the optimization method to ascertain true values for the other two parameters.

This method is subject to several limitations. First, the optimization problem was formulated with the assumption, in accordance with traditional inverse dynamics studies, that each segment in the body could be viewed as a rigid link. Yet, in reality, the segments consist of two parts: bones, which are considered rigid, and soft tissues (e.g., muscle, skin, and ligament), which are not. Therefore, researchers have concluded that during high-impact motions, the rigid body model may not be suitable [37]. Thus, due to the rigid body assumption, the calibration motions should be based on relatively slow motions with no impact. Second, in this investigation we did not consider the effects of inaccuracies in GRF measurements on the net joint torque estimations. Third, our method may not be suitable for finding BSP for small body parts (e.g., fingers) since these have relatively small effects on the ground reaction forces. Fourth, in cases where the initial BSP estimates are very close to the true values, it is possible that the optimized BSP after step 1 will be slightly worse (e.g., lines 3 and 7 in Table 2). This issue is also one reason for adding the second optimization step since after step 2 the error is very small.

A final limitation is that this study used a 2D model with three degrees of freedom (3DOFs) to represent the human musculoskeletal system. Therefore, currently this method only supports BSP estimations in the sagittal plane. Also, the body was represented by three segments with the assumption that bilateral motion and BSP were symmetrical. Real experiments, on the other hand, may require more than three segments to represent human motion, and the symmetry assumption for the body segments may not be valid. In such cases, more complex models (with more degrees of freedom and more optimization variables) will be needed. The 3DOF problem presented in this paper has ~350 variables. More complex problems will likely range from 1000 to 3000 variables. Even with these large numbers, it should be quite feasible to implement this optimization approach in the future as the optimization problem scales roughly linearly, and problems with 500–5000 variables are not considered especially "large" given current computational capabilities [38].

Future studies should be conducted to extend the proposed approach to account for inaccuracies in the ground reaction measurements and to add more DOF to the model (in 2D and 3D). For example, this technique may be applicable to data collection situations when two force plates are used. One adaptation could be to create two inverse dynamics models: a bottom-up model for the lower extremities that uses the ground reaction data and a top-down model for the upper extremities. These models would then meet at some point on the torso (e.g., L5/S1 joint). The optimization would adjust parameters in the each model in order to minimize the difference in the forces and torque at this meeting point. An additional improvement could be to include an iterative cycle in which the refined BSP after step 2 (BSP2) would be used to calculate new estimations of the angular profile for each of the three calibration motions. Optimal BSP estimates could then be achieved by repeating the iteration until convergence. As an alternative method for achieving better motion profile estimations, corrective methods that compensate for skin movement artifacts, such as the cluster method [39] and global optimization methods incorporating joint kinematics constraints [33–35], could then be used in step 2 to optimize for BSP.

In summary, this research built upon a method proposed by Vaughan et al. [17] that attempts to improve net joint torque accuracy by optimization of the BSP. Our method enables estimation of the body segment parameters while characteristic errors in motion measurements are present. The results of our approach significantly reduced the errors in the inverse dynamics solutions for net joint torques due to BSP inaccuracies when compared to the results of initial estimates. Full development of this method can lead to a simple fast technique for improving inverse dynamics-based net joint torque calculations through the use of a series of short calibration motions. By applying the optimization approach

to these calibration motions, it is possible to identify a set of BSP for a given individual. These BSP values would then be used in inverse dynamics analyses of desired experimental motion(s) performed by the subject. While knowledge in optimization techniques is currently necessary to further explore this method, we envision a future where optimization methods for improving estimations for BSP, motion profiles, joint torques, etc., will be provided by motion-capture system manufacturers or third-party biomechanics companies in the same manner that they currently provide programs to calculate 2D/3D joint torque and angle data.

Acknowledgment

We thank Professor Placid Ferreira for assistance with optimization concepts and Alex Shorter for help in conducting the experiments and constructive comments.

References

[1] Winter, D. A., 2005, *Biomechanics and Motor Control of Human Movement*, Wiley, Hoboken, NJ.
[2] Riemer, R., Hsiao-Wecksler, E. T., and Zhang, X., 2008, "Uncertainties in Inverse Dynamics Solutions: A Comprehensive Analysis and an Application to Gait," Gait and Posture, **27**(4), pp. 578–588.
[3] Leardini, A., Chiari, L., Croce, U. D., and Cappozzo, A., 2005, "Human Movement Analysis Using Stereophotogrammetry: Part 3: Soft Tissue Artifact Assessment and Compensation," Gait and Posture, **21**(2), pp. 212–225.
[4] Cappozzo, A., and Berme, N., 1990, Biomechanics of Human Movement Applications in Rehabilitation, Sports and Ergonomics, Worthington, OH, Bertec Corporation, Subject Specific Segment Inertial Parameter Determination: A Survey of Current Methods.
[5] Challis, J. H., 1996, "Accuracy of Human Limb Moment of Inertia Estimations and Their Influence on Resultant Joint Moments," J. Appl. Biomech., **12**(4), pp. 517–530.
[6] Ganley, K. J., and Powers, C. M., 2004, "Determination of Lower Extremity Anthropometric Parameters Using Dual Energy X-Ray Absorptiometry: The Influence on Net Joint Moments During Gait," Clin. Biomech. (Bristol, Avon), **19**(1), pp. 50–56.
[7] Kingma, I., Toussaint, H. M., De Looze, M. P., and Van Dieen, J. H., 1996, "Segment Inertial Parameter Evaluation in Two Anthropometric Models by Application of a Dynamic Linked Segment Model," J. Biomech., **29**(5), pp. 693–704.
[8] Dempster, W., T, 1955, "Space Requirements of Seated Operator," Aerospace Medical Research Laboratories, Technical Report No. WADC-TR-55-159.
[9] De Leva, P., 1996, "Adjustments to Zatsiorsky-Seluyanov's Segment Inertia Parameters," J. Biomech., **29**(9), pp. 1223–1230.
[10] Durkin, J. L., and Dowling, J. J., 2003, "Analysis of Body Segment Parameter Differences Between Four Human Populations and the Estimation Errors of Four Popular Mathematical Models," ASME J. Biomech. Eng., **125**((4)), pp. 515–522.
[11] Zatsiorsky, V., Seluyanov, V., and Chugunova, L. G., 1990, "Contemporary Problems of Biomechanics," *Methods of Determining Mass-Inertial Characteristics of Human Body Segments*, CRC Press, Boston.
[12] Hatze, H., 1980, "A Mathematical Model for the Computational Determination of Parameter Values of Anthropomorphic Segments," J. Biomech., **13**(10), pp. 833–843.
[13] Yeadon, M. R., 1990, "The Simulation of Aerial Movement—II. A Mathematical Inertia Model of the Human Body," J. Biomech., **23**(1), pp. 67–74.
[14] Durkin, J. L., James, J. D. B., and Andrews, D. M., 2002, "The Measurement of Body Segment Inertial Parameters Using Dual Energy X-Ray Absorptiometry," J. Biomech., **35**(12), pp. 1575–1580.
[15] Zatsiorsky, V. M., and Seluyanov, V. N., 1983, "The Mass and Inertia Characteristics of the Main Segments of the Human Body," *Biomechanics VIII-B*, Human Kinetics, Champaign, IL.
[16] Kodek, T., and Munih, M., 2006, "An Identification Technique for Evaluating Body Segment Parameters in the Upper Extremity from Manipulator-Hand Contact Forces and Arm Kinematics," Clin. Biomech. (Bristol, Avon), **21**(7), pp. 710–716.
[17] Vaughan, C. L., Andrews, J. G., and Hay, J. G., 1982, "Selection of Body Segment Parameters by Optimization Methods," ASME J. Biomech. Eng., **104**(1), pp. 38–44.
[18] Cahouet, V., Luc, M., and David, A., 2002, "Static Optimal Estimation of Joint Accelerations for Inverse Dynamics Problem Solution," J. Biomech., **35**(11), pp. 1507–1513.
[19] Kuo, A. D., 1998, "A Least-Squares Estimation Approach to Improving the Precision of Inverse Dynamics Computations," ASME J. Biomech. Eng., **120**(1), pp. 148–159
[20] Delp, S. L., Anderson, F. C., Arnold, A. S., Loan, P., Habib, A., John, C. T., Guendelman, E., and Thelen, D. G., 2007, "Opensim: Open-Source Software to Create and Analyze Dynamic Simulations of Movement," IEEE Trans. Biomed. Eng., **54**(11), pp. 1940–1950.
[21] Cappozzo, A., 2002, "Minimum Measured-Input Models for the Assessment of Motor Ability," J. Biomech., **35**(4), pp. 437–446.
[22] Mazza, C., and Cappozzo, A., 2004, "An Optimization Algorithm for Human Joint Angle Time-History Generation Using External Force Data," Ann. Biomed. Eng., **32**(5), pp. 764–772.
[23] Cappozzo, A., Catani, F., Leardini, A., Benedetti, M. G., and Della Croce, U., 1996, "Position and Orientation in Space of Bones During Movement: Experimental Artefacts," Clin. Biomech. (Bristol, Avon), **11**(2), pp. 90–100.
[24] Holden, J. P., Orsini, J. A., Siegel, K. L., Kepple, T. M., Gerber, L. H., and Stanhope, S. J., 1997, "Surface Movement Errors in Shank Kinematics and Knee Kinetics During Gait," Gait and Posture, **5**(3), pp. 217–227.
[25] Stagni, R., Fantozzi, S., Cappello, A., and Leardini, A., 2005, "Quantification of Soft Tissue Artefact in Motion Analysis by Combining 3D Fluoroscopy and Stereophotogrammetry: A Study on Two Subjects," Clin. Biomech. (Bristol, Avon), **20**(3), pp. 320–329.
[26] Richards, J. G., 1999, "The Measurement of Human Motion: A Comparison of Commercially Available Systems," Hum. Mov. Sci., **18**(5), pp. 589–602
[27] Bell, A. L., Pedersen, D. R., and Brand, R. A., 1990, "A Comparison of the Accuracy of Several Hip Center Location Prediction Methods," J. Biomech., **23**(6), pp. 617–621.
[28] Leardini, A., Cappozzo, A., Catani, F., Toksvig-Larsen, S., Petitto, A., Sforza, V., Cassanelli, G., and Giannini, S., 1999, "Validation of a Functional Method for the Estimation of Hip Joint Centre Location," J. Biomech., **32**(1), pp. 99–103.
[29] Roux, E., Bouilland, S., Godillon-Maquinghen, A. P., and Bouttens, D., 2002, "Evaluation of the Global Optimisation Method Within the Upper Limb Kinematics Analysis," J. Biomech., **35**(9), pp. 1279–1283.
[30] Schwartz, M. H., and Rozumalski, A., 2005, "A New Method for Estimating Joint Parameters From Motion Data," J. Biomech., **38**(1), pp. 107–116.
[31] Riemer, R., and Hsiao-Wecksler, E. T., 2008, "Optimization-Based Inverse Dynamics to Reduce the Effect of Motion Errors in Joint Torque Calculations," J. Biomech., **41**(7), pp. 1503–1509.
[32] Chaffin, B. D., Gunnar, B. J. A., and Martin, B., 1999, *Occupational Biomechanics*, Wiley, New York.
[33] Cheze, L., Fregly, B. J., and Dimnet, J., 1995, "A Solidification Procedure to Facilitate Kinematic Analyses Based on Video System Data," J. Biomech., **28**(7), pp. 879–884.
[34] Lu, T. W., and O'Connor, J. J., 1999, "Bone Position Estimation From Skin Marker Co-Ordinates Using Global Optimisation With Joint Constraints," J. Biomech., **32**(2), pp. 129–134.
[35] Reinbolt, J. A., Schutte, J. F., Fregly, B. J., Koh, B. I., Haftka, R. T., George, A. D., and Mitchell, K. H., 2005, "Determination of Patient-Specific Multi-Joint Kinematic Models Through Two-Level Optimization," J. Biomech., **38**(3), pp. 621–626.
[36] Block, D. J., and Spong, M. W., 1995, *Mechanical Design and Control of the Pendubot*, Peoria, IL, pp. 1–4.
[37] Gruber, K., Denoth, J., Stuessi, E., and Ruder, H., 1987, "The Wobbling Mass Model," *Biomechanics X-B*, B. Jonsson, ed., Human Kinetics, Champaign, IL.
[38] Saunders, M. A., 2008 private communication.
[39] Alexander, E. J., and Andriacchi, T. P., 2001, "Correcting for Deformation in Skin-Based Marker Systems," J. Biomech., **34**(3), pp. 355–361.